Article

Current Biology

Rocking Promotes Sleep in Mice through Rhythmic Stimulation of the Vestibular System

Graphical Abstract

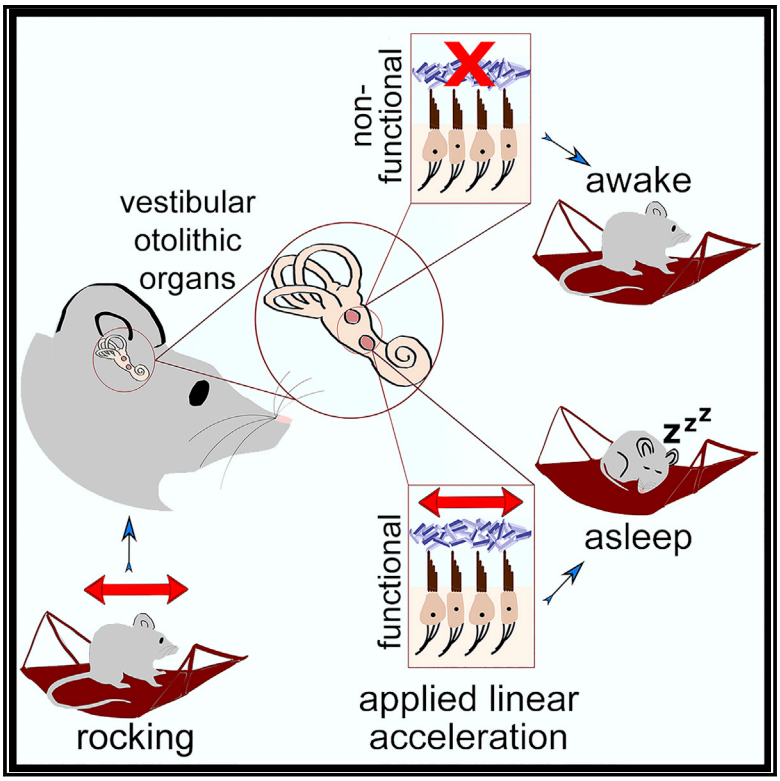

Authors

Konstantinos Kompotis,
Jeffrey Hubbard,
Yann Emmenegger, ...,
Sophie Schwartz, Laurence Bayer,
Paul Franken

Correspondence

paul.franken@unil.ch

In Brief

Kompotis et al. demonstrate for the first time that rocking promotes sleep in a species other than the human: i.e., the mouse. They also provide the first evidence that the vestibular otolithic organs mediate sleep promotion and that this effect depends on the linear acceleration applied, and not on the rocking frequency.

Highlights

- Rhythmic mechanosensory stimulation (aka rocking) promotes sleep also in the mouse
- Linear acceleration applied to the head encodes the rocking stimulus
- The rocking effects on sleep are acceleration and time specific
- The otolithic organs of the vestibular system mediate the rocking effects on sleep

Kompotis et al., 2019, Current Biology *29*, 392–401
February 4, 2019
https://doi.org/10.1016/j.cub.2018.12.007

CellPress

CellPress

Current Biology
Article

Rocking Promotes Sleep in Mice through Rhythmic Stimulation of the Vestibular System

Konstantinos Kompotis,[1] Jeffrey Hubbard,[1] Yann Emmenegger,[1] Aurore Perrault,[2,3] Michel Mühlethaler,[2] Sophie Schwartz,[2,3] Laurence Bayer,[2,4,5] and Paul Franken[1,5,6,*]

[1]Center for Integrative Genomics, Faculty of Biology and Medicine, University of Lausanne, 1015 Lausanne, Switzerland
[2]Department of Basic Neurosciences, Faculty of Medicine, University of Geneva, 1211 Geneva, Switzerland
[3]Swiss Center for Affective Science, Campus Biotech, 1202 Geneva, Switzerland
[4]Center for Sleep Medicine, Geneva University Hospital, 1225 Geneva, Switzerland
[5]These authors contributed equally
[6]Lead Contact
*Correspondence: paul.franken@unil.ch
https://doi.org/10.1016/j.cub.2018.12.007

SUMMARY

Rocking has long been known to promote sleep in infants and, more recently, also in adults, increasing NREM sleep stage N2 and enhancing EEG slow waves and spindles. Nevertheless, whether rocking also promotes sleep in other species, and what the underlying mechanisms are, has yet to be explored. In the current study, C57BL/6J mice equipped with EEG and EMG electrodes were rocked laterally during their main sleep period, i.e., the 12-h light phase. We observed that rocking affected sleep in mice with a faster optimal rate than in humans (1.0 versus 0.25 Hz). Specifically, rocking mice at 1.0 Hz increased time spent in NREM sleep through the shortening of wake episodes and accelerated sleep onset. Although rocking did not increase EEG activity in the slow-wave and spindle-frequency ranges in mice, EEG theta activity (6–10 Hz) during active wakefulness shifted toward slower frequencies. To test the hypothesis that the rocking effects are mediated through the vestibular system, we used the otoconia-deficient *tilted* (*tlt*) mouse, which cannot encode linear acceleration. Mice homozygous for the *tlt* mutation were insensitive to rocking at 1.0 Hz, while the sleep and EEG response of their heterozygous and wild-type littermates resembled those of C57BL/6J mice. Our findings demonstrate that rocking also promotes sleep in the mouse and that this effect requires input from functional otolithic organs of the vestibule. Our observations also demonstrate that the maximum linear acceleration applied, and not the rocking rate per se, is key in mediating the effects of rocking on sleep.

INTRODUCTION

The beneficial influence of rhythmic passive movement, widely known as rocking, on human sleep constitutes a familiar phenomenon, especially in early infancy. The first systematic studies on infants confirmed that rocking increased sleep duration, decreased motor activity during waking, and shortened sleep-onset latency [1–3]. In an early study investigating the effects of rocking in adults, a tendency toward a shorter latency to sleep onset after three nights and a decrease in non-rapid eye movement (NREM) stage 2 (N2) were observed [4]. More recently, healthy adult subjects rocked laterally during a single afternoon nap showed reduced sleep-onset latency, increased N2 duration, and enhanced electroencephalographic (EEG) markers of sleep quality [5]. Conversely, Omlin and colleagues, testing various planes of motion and rocking rates with a rhythmically moving bed, did not observe any influence of rocking on adult sleep [6, 7]. Of note, rocking conditions, such as the duration, rate, and displacement, differed among the three studies.

Despite several efforts to document the impact of rocking on sleep, the underlying mechanisms remain elusive. For instance, whether the effects observed on adult sleep are an all-or-nothing or a dose-dependent phenomenon has not yet been conclusively addressed [7]. Furthermore, although it is generally assumed that the effects of rocking are conveyed through the vestibular system [3, 4, 8], its direct involvement and the respective contributions of the various vestibular organs (reviewed in [9]) remain to be experimentally verified. Moreover, the contribution of other sensory modalities capable of encoding passive movement [10, 11], such as the proprioceptive and visual systems, to the effects of rocking on sleep remains unexplored. Finally, whether rocking affects sleep in species other than humans has never before been addressed.

The present study aimed at elucidating the mechanism underlying the effects of rocking on sleep. To this end, we first established a mouse model of rocking and found that rocking, by means of rhythmic linear acceleration in the horizontal plane, affected sleep time, sleep architecture, and EEG activity in an acceleration- and time-dependent manner. At the optimal applied acceleration, mice spent more time in NREM sleep and fell asleep faster, and their theta (6–10 Hz) EEG activity during wakefulness shifted toward slower frequencies. The involvement of the vestibular system in mediating the effect was assessed by using B6.Cg-*Otop1*tlt/J (*Otop1*) *tilted* mice, which lack functional otoliths and thus are unable to encode linear acceleration

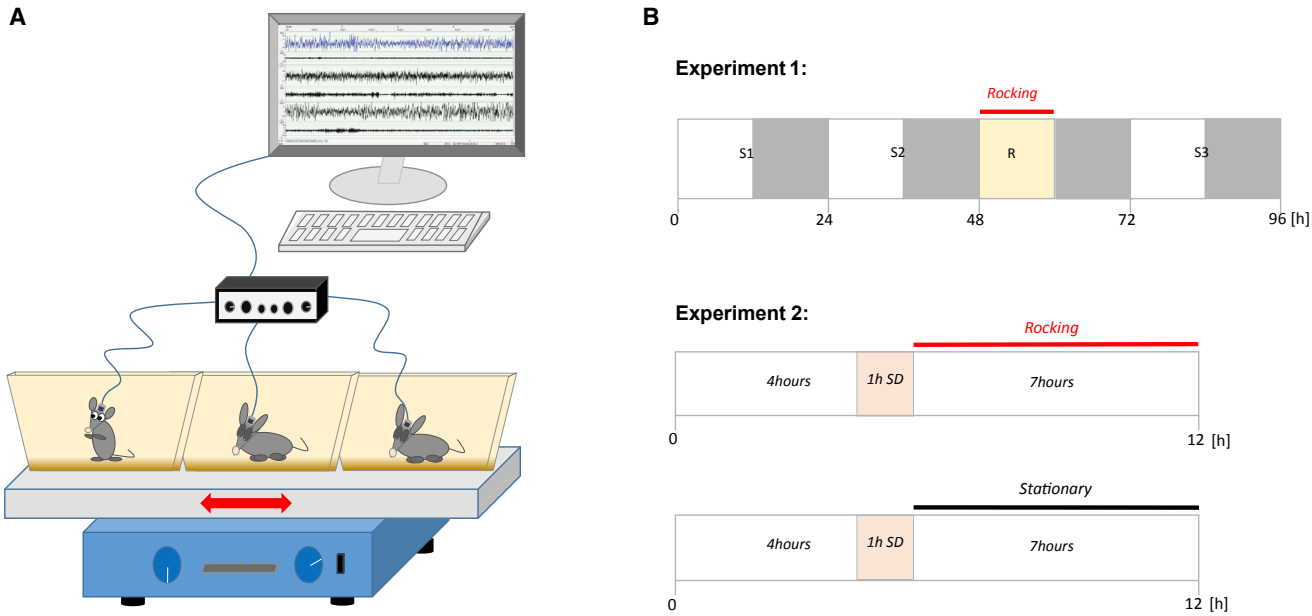

Figure 1. Schematic of the Rocking Setup and Experimental Design

(A) Individually housed mice were placed on a laterally moving platform. Mice were implanted with EEG and EMG electrodes and connected through a cable to the recording unit. EEG and EMG signals were visualized, stored, and analyzed on a computer.

(B) Experiment 1 (upper panel) consisted of a 48-h baseline recording (stationary days S1 and S2), followed by 12 h of rocking (R) during the light period (ZT0–ZT12). During the ensuing dark period (ZT12–ZT24) and the last recording day (S3), mice were not rocked. Experiment 2 (lower panel) assessed the effects of rocking on sleep-onset latency. Mice were left undisturbed until ZT4 and were then sleep deprived (SD) for 1 h (ZT4–ZT5) and subsequently left to sleep under stationary or rocking condition during the remainder of the light period (ZT5–ZT12).

[12, 13]. The effects of rocking on sleep architecture and EEG activity were noticeably absent in *tilted* mice, thereby demonstrating that the vestibular otolithic organs mediate the sleep-promoting effects of rocking.

RESULTS

In the current study, rocking motion was simulated through a platform moving rhythmically in the horizontal plane (Figure 1A). To establish the optimal rocking rate, we first rocked C57BL6/J mice at 0.25 Hz, the rate used in humans by Bayer and colleagues [5], and then at 0.5, 1.0, and 1.5 Hz, using a within-subject design and controlling for possible order effects. A 2.0-Hz rocking rate was tested as well, but it was quickly abandoned as it caused obvious discomfort to the mice. Each experiment consisted of a 4-day recording, and mice were rocked during the 12-h light period of the third day (Figure 1B, experiment 1).

Rocking Affects Sleep in a Rate- and Time-Specific Manner

Rocking at 0.25 and 0.5 Hz did not affect the sleep-wake distribution when compared to the stationary baseline condition (days S1 and S2) or the following stationary day (day S3; Figures 2A, and 2B). Conversely, rocking at 1.0 and 1.5 Hz promoted NREM sleep (Figures 2A and 2B). During the 12-h rocking at 1.0 Hz, mice gained a total of 48.4 ± 5.9 min of NREM sleep (i.e., +12% of stationary baseline NREM sleep; Figure 2B, upper-left panel). This gain was accrued mainly within the first 3 h after the rocking onset (ZT0–ZT3; 26.7 ± 3.0 min, i.e., +25% compared to corresponding baseline hours; Figure 2A). Rocking at 1.5 Hz increased NREM-sleep time by 85.5 ± 10.5 min (+21% over baseline; Figure 2B, upper-left panel). This effect was most prominent during ZT2–ZT7, as well as at the end of the light period (Figure 2A). Interestingly, NREM sleep was still increased for the first 3 h of the subsequent dark period (ZT12–ZT15), when rocking was no longer applied. Nevertheless, NREM sleep over the 12-h dark period did not differ from the baseline (Figure 2A; Figure S1B, left panel).

NREM-sleep gain during 1.0-Hz rocking was at the sole expense of wakefulness, as time spent in rapid eye movement (REM) sleep remained unaltered (Figure 2B, upper-right panel). In addition to reducing wakefulness, rocking at 1.5 Hz resulted, however, in a 20% reduction of REM sleep (−11.0 ± 3.9 min from baseline; Figure 2B, upper-right panel; Table S1). This suppression of REM sleep was followed by a rebound of +8.8 ± 2.2 min (+79%) during the subsequent dark period (Figure S1B, right panel), recovering 80% of REM sleep lost during the preceding light period. The sleep-wake distribution during stationary day S3 was not affected at either rocking rate.

NREM and REM sleep each contributed to total sleep (TS) at relatively constant ratios during the baselines of 1.0- and 1.5-Hz rocking (for REM-sleep/TS ratios, see Table S1). As NREM-sleep time, but not REM-sleep time, increased during 1.0-Hz rocking, the relative contribution of REM sleep to TS decreased significantly from 0.12 to 0.11, i.e., an 11% decrease compared to stationary levels (Figure 2B, bottom-left panel). A profound reduction in the REM-sleep/TS ratio was observed at 1.5 Hz (from 0.12 to 0.09; a 31% decrease; Figure 2B,

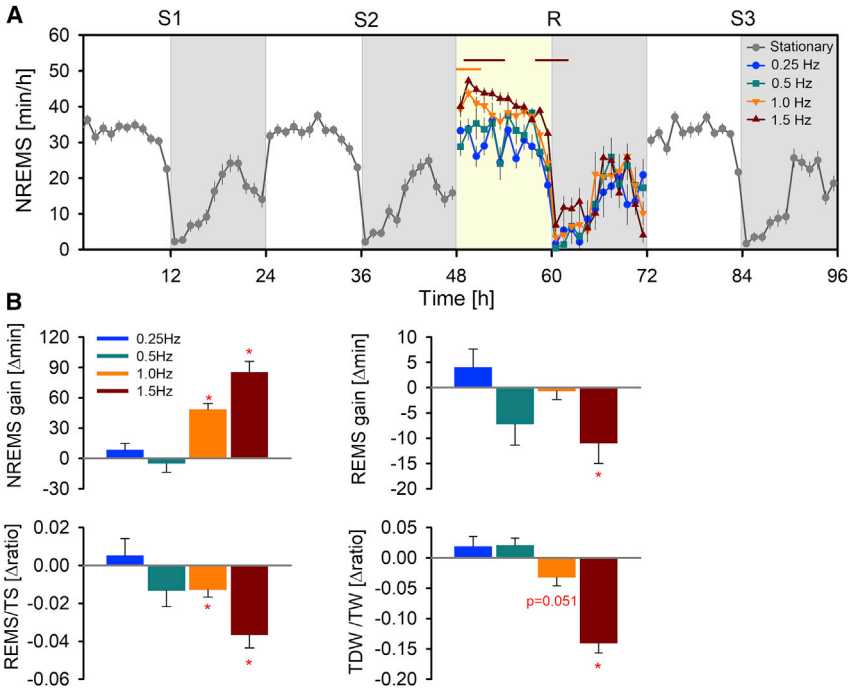

Figure 2. Effects of Rocking Rate on the Sleep-Wake Distribution

(A) NREM-sleep (NREMS; mean minutes/hour ± 1 SEM) time course during stationary (S1, S2, and S3; gray symbols and line; averaged over all four rocking experiments; for individual values, see Figure S1A) and rocking (R) conditions at 0.25 (blue), 0.5 (green), 1.0 (orange), and 1.5 Hz (dark red). Animals were rocked only during the 12-h light period (yellow area within day R). The gray areas represent 12-h dark periods. Significant rocking-stationary (mean of S1/S2 12-h light periods) differences are depicted by orange (1.0 Hz) and dark-red (1.5 Hz) horizontal lines above graphs (2-way rANOVA, condition, $p < 0.002$; post hoc paired t tests, $p < 0.05$; $n_{0.25\ Hz} = 6$, $n_{0.5\ Hz} = 7$, $n_{1.0\ Hz} = 9$, $n_{1.5\ Hz} = 9$).

(B) Average (±1 SEM) rocking-stationary differences in time spent asleep (NREMS, upper-left panel; REMS, upper-right panel), REMS as a ratio of total sleep time (REMS/TS; lower-left panel), and theta-dominated waking as a ratio of total time spent awake (TDW/TW; lower-right panel) over the 12-h light period for the 4 rocking rates (for a definition of TDW, see STAR Methods). The values are expressed in Δminutes per 12 h for the upper two panels and in Δratio for the left- and right-lower panels, respectively (see Table S1). Also see Figures S1B and S6 for NREMS and REMS differences in the dark period and at 1.0 Hz with different displacements, respectively. The red asterisks mark significant differences between the 2 conditions (1-way ANOVA, rocking rate, $p < 0.025$; paired t test, stationary versus rocking, $p < 0.001$; for all states, $n_{0.25\ Hz} = 6$, $n_{0.5\ Hz} = 7$, $n_{1.0\ Hz} = 9$, $n_{1.5\ Hz} = 9$, except for TDW, $n_{0.25\ Hz} = 3$, $n_{0.5\ Hz} = 7$, $n_{1.0\ Hz} = 8$, $n_{1.5\ Hz} = 9$, due to exclusion of mice with waking EEG artifacts precluding TDW determination [see STAR Methods]).

bottom-left panel). This result indicates that rocking favors NREM sleep specifically, at the cost of both REM sleep and wakefulness.

Rocking has been reported to reduce motor activity during wakefulness in infants [8]. Since waking can be further divided into substates with distinct behavioral and EEG activities [14], we investigated whether rocking specifically targeted a theta-dominated subtype of wakefulness (see STAR Methods), strongly associated with purpose-driven behavior and locomotion in mice [14, 15]. Although no effect was observed at lower rocking rates, 1.0-Hz rocking significantly decreased time spent in theta-dominated waking (−18.0 ± 3.1 min). Rocking at 1.5 Hz decreased theta-dominated waking to a larger extent (−45.9 ± 4.9 min; Table S1) and reduced its contribution to total wakefulness (TW; TDW/TW ratio; from 0.25 to 0.11 or 57% of the stationary condition; Figure 2B).

Thus, an effect of rocking on the sleep-wake distribution was observed only at the two higher rocking rates, with the highest applied rate having a larger impact on NREM-sleep promotion, on theta-dominated wakefulness, and on REM-sleep suppression.

Rocking at 1.5 Hz Negatively Impacts EEG Markers of Sleep Quality

To assess whether rocking induced deeper NREM sleep, we quantified NREM-sleep EEG delta power (1–4 Hz), a proxy of homeostatic sleep pressure correlating well with sleep intensity [16, 17]. Only rocking at 1.5 Hz affected EEG delta power (Figure 3A); within the first 4 h (ZT0–ZT4), EEG delta power was significantly decreased, e.g., from 145% under stationary conditions to 105% under rocking conditions in the first interval (Figure 3A). The reduction in EEG activity was not specific to the delta frequencies and was observed at higher frequencies as well, particularly around the sigma band (11–15 Hz; Figure 3B). NREM-sleep EEG sigma power is associated with occurrence of spindle events [18]. We therefore examined the effects of rocking on the number and timing of discrete surges in sigma power (referred to as "spindles" hereafter; Figure S3A; STAR Methods). The decrease in NREM-sleep sigma power at 1.5-Hz rocking was accompanied by a decrease in spindle density (Figure S3C). Although we could confirm that spindle occurrence is high immediately prior to REM-sleep onset [19] (Figure S3B), analyses of inter-spindle intervals revealed that the timing of spindles was not associated with the rocking rate (Figure S3D).

Although rocking at 1.5 Hz maximally promoted NREM-sleep time, the pronounced suppression of NREM-sleep EEG activity and time spent in REM sleep indicated that sleep was actually disturbed. We will therefore further present only the effect of 1.0-Hz rocking in subsequent analyses and experiments, as we consider this the optimal rocking rate promoting sleep in mice.

Rocking Alters EEG Activity in the Theta Range during Wakefulness

Further analysis demonstrated that 1.0-Hz rocking affected the spectral composition of both the wakefulness and REM-sleep EEG. During total wakefulness, spectral power in the 0.75- to 1.75-Hz, 3.5- to 4.5-Hz, and 8.25- to 12.0-Hz bands decreased, while activity in the 5.5- to 6.25-Hz range increased (Figure 4A, upper-left panel; Figure S2, upper-right panel). In the

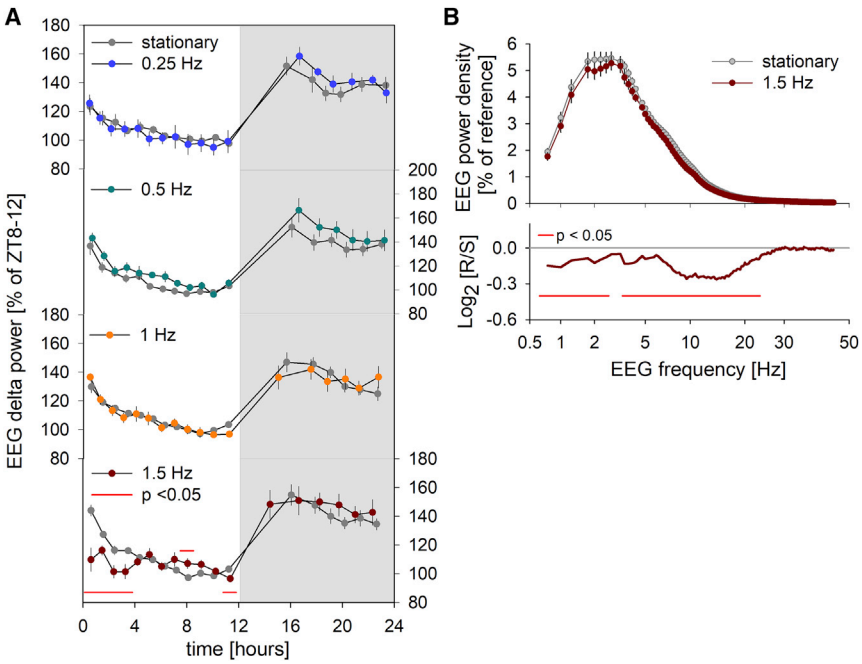

Figure 3. Effects of Rocking on EEG Delta Power

(A) From top to bottom: time course of NREM sleep (NREMS) EEG delta power (1–4 Hz) during rocking (blue, green, orange, and dark-red symbols for 0.25, 0.5, 1.0, and 1.5 Hz, respectively) and stationary (gray symbols) conditions. The gray areas represent 12-h dark periods. The values are expressed as mean percentages (±1 SEM) of the last 4 h of the 2 baseline light periods (ZT8–ZT12; see STAR Methods). Significant differences between conditions are indicated by the red line (2-way rANOVA, time × condition, $p < 0.001$; post hoc paired t tests, $p < 0.05$; $n_{0.25\ Hz} = 6$, $n_{0.5\ Hz} = 7$, $n_{1.0\ Hz} = 8$, $n_{1.5\ Hz} = 9$).

(B) Upper panel: mean NREMS EEG spectral profiles (±1 SEM) during the 12-h light period under stationary (gray line and symbols) and 1.5-Hz rocking (dark-red line and symbols) conditions. The values are expressed as percentages of the baseline reference (S1 and S2; see STAR Methods). The EEG power density values at the 1.5- and 3.0-Hz frequency bins were removed because of technical artifacts (see STAR Methods). Also see Figure S2 for NREMS spectral changes at other rocking rates and Figure S3 for changes in spindle events during NREMS. Lower panel: relative changes for 1.5-Hz rocking (dark-red line) versus stationary (gray horizontal line at 0) conditions, expressed as the $\log_2$ of the rocking/stationary ratio. The red horizontal lines connect frequency bins in which rocking affected the EEG power density (2-way rANOVA, condition, $p = 0.003$; frequency × condition, $p < 0.001$; post hoc paired t tests, $p < 0.05$; $n = 9$).

theta-dominated waking EEG (Figure 4A, lower-right panel), a similar decrease was observed in the 0.75- to 1.75- and 8.75- to 11.75-Hz range, whereas an increase in power was noted in the 6.5- to 7.25-Hz frequency band. The increased power surrounding the lower theta frequency range (5.25–7.5 Hz) was also observed in REM sleep (Figure 4A, upper-right panel), during which, in addition, an increase throughout the beta and low-gamma (15–45 Hz) ranges was found.

The increase in EEG power in the lower theta range, concomitant with the reduction of power in the higher theta range observed during theta-dominated waking, suggested a shift of the theta peak toward lower frequencies. Indeed, theta peak frequency (TPF, see STAR Methods) during theta-dominated waking was significantly reduced (−0.17 ± 0.02 Hz; Figure 4B). Rocking did not affect TPF in REM sleep.

Rocking Favors Wake-to-NREM Sleep Transitions

To assess the effects of 1.0-Hz rocking on sleep-wake continuity, we quantified the number and length of waking, NREM-sleep, and REM-sleep episodes. Rocking reduced waking-episode length, while a non-significant tendency toward shorter NREM-sleep episodes was observed (Figure 5A). During rocking, both waking and NREM-sleep episodes occurred more often (+25% for both; Figure 5B). These effects were amplified at 1.5-Hz rocking (+62% for both states; Figure S4), with a concomitant significant reduction in NREM-sleep episode duration and the number of REM-sleep episodes. These observations suggest that during 1.0-Hz rocking, the overall increase in NREM-sleep time was primarily due to wake-to-NREM sleep transitions being favored. Although 1.5-Hz rocking did increase overall time spent in NREM sleep, this sleep state was more fragmented through an increase in the number of awakenings precluding transitions into REM sleep. This result further attests to the fact that at this rate, rocking disrupts sleep.

Although exceptions can be found [7], rocking was reported to shorten sleep-onset latency in humans [4, 5, 20]. To assess the rocking effect on sleep-onset latency, we sleep deprived mice for 1 h (ZT4–ZT5), which was followed either by 7 h of rocking or a stationary condition (see STAR Methods and Figure 1B, experiment 2). Rocking at 1.0 Hz reduced sleep-onset latency by 11.0 ± 1.3 min (51%) when compared to the stationary condition (Figure 5C), corroborating the observations in humans and further supporting the facilitation of transitions into NREM sleep.

Mice with Defective Otoliths Are Insensitive to the Effects of Rocking on Sleep

In the second part of the study, we addressed the hypothesis that the otolithic organs of the vestibular system mediate the rocking effects on sleep using B6.Cg-*Otop1*tlt/J *tilted* (*Otop1*$^{tlt/tlt}$) mice. These mice cannot encode linear acceleration due to their lack of functional otoliths, while they exhibit no apparent abnormal phenotype in other sensory organs [12, 21].

Tilted mice, and their heterozygous (*Otop1*$^{+/tlt}$) and wild-type (*Otop1*$^{+/+}$) littermates, were rocked at 1.0 Hz according to experiment 1 (Figure 1B). Baseline NREM-sleep amounts (Figure S5A; Table S2) and EEG spectral profiles (Figure S5B) were similar among the three *Otop1* genotypes, suggesting that otoliths are not necessary for physiological sleep under undisturbed conditions.

Similar to the B6 group (Figure 2B), both *Otop1*$^{+/+}$ (+44.3 ± 5.1 min) and *Otop1*$^{+/tlt}$ (+39.0 ± 8.7 min) mice experienced an increase in NREM sleep at 1.0 Hz (Figure 6A, left panel), at the

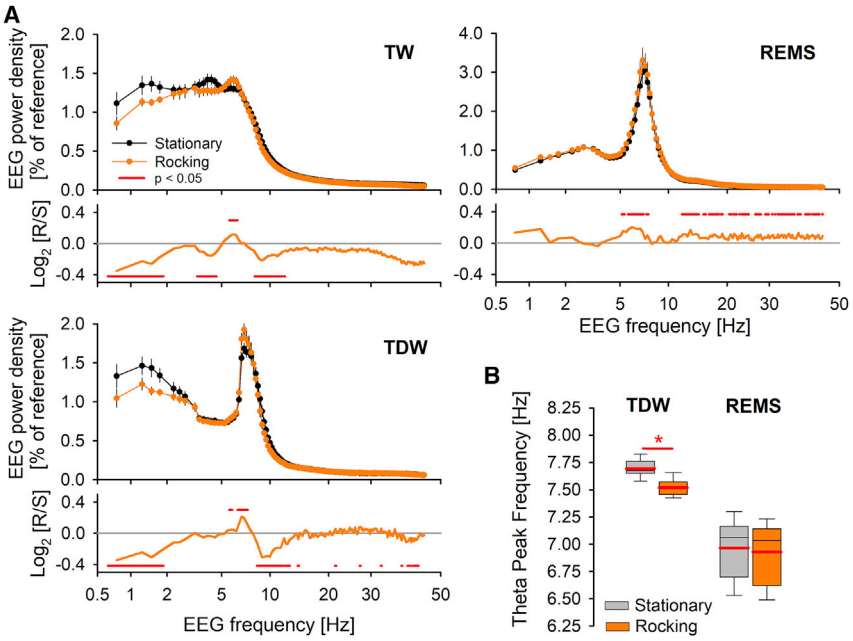

Figure 4. Rocking at 1.0 Hz Affects the EEG during Wakefulness and REMS

(A) Mean EEG spectral profiles (±1 SEM) of total wakefulness (TW; upper-left panel), theta-dominated waking (TDW; bottom-left panel), and REM sleep (REMS; upper-right panel) during the 12-h light period under stationary (black line and symbols) and 1.0-Hz rocking (orange line and symbols) conditions. The values are expressed as percentages of the baseline reference (S1 and S2; see STAR Methods). EEG power densities at 1.0, 2.0, and 3.0 Hz were removed because of rocking artifacts in some mice (see STAR Methods). See Figure S2 for EEG changes at other rocking rates. Below each panel, the respective relative changes for rocking at 1.0-Hz (orange line) versus stationary (gray horizontal line at 0) conditions, expressed as the $\log_2$ of the rocking/stationary ratio. For TW (2-way rANOVA, frequency × condition, $p < 0.001$), TDW (2-way rANOVA, frequency × condition, $p < 0.001$), and REMS (2-way rANOVA, condition, frequency × condition, $p < 0.001$), significantly different frequency bins between the two conditions are marked by the red squares (post hoc paired t tests, $p < 0.05$; $n = 8$).

(B) Theta peak frequency during TDW and REMS under rocking and stationary conditions (see STAR Methods). The gray and orange boxplots represent the stationary and rocking conditions, respectively. The mean and median of each condition are indicated by the red and black lines, respectively. The error bars span the 5th to 95th percentiles. The red asterisk marks significant stationary versus rocking differences (paired t test, $p = 1.3 \times 10^{-5}$, $n_{TDW} = 8$, $n_{REMS} = 8$).

expense of wakefulness, with no alteration in REM-sleep time (Figure 6A, second-left panel). However, when expressed as a ratio of TS, REM sleep did again significantly decrease (from 0.14 to 0.12 [−13%] and from 0.15 to 0.14 [−8%], in *Otop1*$^{+/+}$ and *Otop1*$^{+/tlt}$, respectively; Figure 6A, third-left panel). Also, the theta-dominated waking/total wakefulness ratio decreased significantly in both *Otop1*$^{+/+}$ and *Otop1*$^{+/tlt}$ mice (from 0.18 to 0.12 [−37%] and from 0.19 to 0.13 [−29%], respectively; Figure 6A, right panel; Table S2), diverging from the non-significant theta-dominated waking/total wakefulness ratio decrease from 0.23 to 0.20, i.e., −14%, in B6 mice (Figure 2B). Conversely, *Otop1*$^{tlt/tlt}$ mice did not respond to rocking, maintaining a similar sleep-wake distribution as they exhibited during the stationary condition (Figure 6A).

Like in B6 mice, rocking reduced the mean duration of waking episodes in *Otop1*$^{+/+}$ (−0.4 ± 0.1 min; −34%) and heterozygous (−0.3 ± 0.0 min; −30%) mice (Figure 6B, left panel) and slightly reduced NREM-sleep episode length only in heterozygous mice (−0.7 ± 0.1 min; −10%). During rocking, the number of waking and NREM-sleep episodes increased in *Otop1*$^{+/+}$ (+33.2% ± 7.3% and +27.2% ± 8.2%, respectively) and *Otop1*$^{+/tlt}$ mice (+19.6% and +19.4%, respectively; Figure 6B, right panel). The length and number of REM-sleep episodes were not affected. *Tilted* mice remained unresponsive to rocking also for these variables (Figure 6B; also see Table S2).

We next investigated sleep-onset latency in the three genotypes (Figure 1B, experiment 2). Rocking shortened sleep-onset latency by 31.0 ± 4.4 min (−60%) in *Otop1*$^{+/+}$ and by 14.9 ± 3.1 min (−41%) in *Otop1*$^{+/tlt}$ mice (Figure 6C), but again did not affect *Otop1*$^{-/-}$ mice. Overall, *Otop1* mice with intact otoliths confirmed the effects of 1.0-Hz rocking on sleep architecture observed in B6 mice, while mice incapable of encoding linear acceleration remained conspicuously unaffected.

Rocking Affects EEG Activity of Wakefulness, Theta-Dominated Waking, and REM Sleep via the Otolithic System

The spectral composition of total wakefulness, theta-dominated waking, and REM-sleep EEG activity was affected by rocking subjects with functional otoliths only, and the effects were strikingly similar to those observed in the B6 mice (Figure 7A). During total wakefulness, EEG power in the 5.5- to 6.5-Hz range increased, while in the 7.25- to 9.25-Hz band, it decreased. A significantly lower EEG power was also noted at 37–45 Hz in both *Otop1*$^{+/+}$ and *Otop1*$^{+/tlt}$ mice (Figure 7A, left panel). In the 2.25- to 3.25-Hz range, EEG activity increased in the *Otop1*$^{+/+}$ and *Otop1*$^{+/tlt}$ mice, similar to the activity in B6 mice when rocked at 1.5 Hz (1.75–3.75 Hz; Figure S2). During theta-dominated waking, *Otop1*$^{+/+}$ and *Otop1*$^{+/tlt}$ mice exhibited a power increase in the 5.5- to 7.25-Hz range and a decrease in the 8.0- to 9.5-Hz range (Figure 7A, middle panel), while a reduction in the 40- to 45-Hz range was also present. In REM sleep, EEG power was higher in the 5.5- to 6.5-Hz range, lower in the 8.5- to 10-Hz range, and higher again in the 30- to 45-Hz range (Figure 7A, right panel) in both genotypes with functional otoliths. Conversely, *Otop1*$^{tlt/tlt}$ mice did not exhibit any consistent difference in their EEG spectral profiles between the two conditions (Figure 7A), extending the observation that rocking affects sleep behavior through the otolithic organs to EEG activity.

Comparison of TPF in theta-dominated waking between the two conditions yielded similar phenotypes in the genotypes with functional otoliths (Figure 7B, left panel; see also Figure 4B).

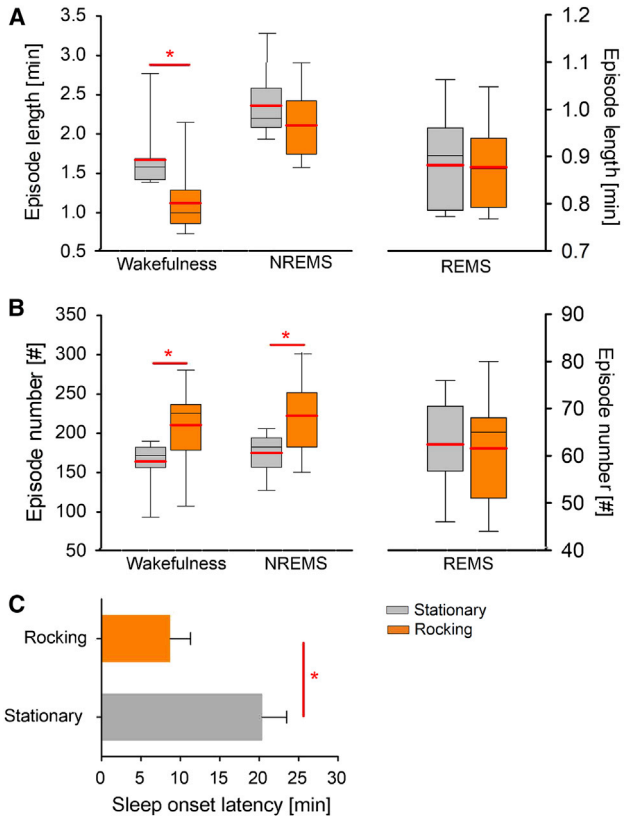

Figure 5. Rocking at 1.0 Hz Increases the Number of NREM-Sleep and Waking Episodes while Shortening Wake-Episode Length and Sleep-Onset Latency

(A) Average episode duration (in minutes) for all 3 states during the 12-h light period (see Figure S4A for changes at 1.5-Hz rocking).

(B) Mean number of uninterrupted episodes for all 3 states during the 12-h light period (see Figure S4B for 1.5-Hz-rocking induced changes). In A and B, the mean and median of each condition are indicated by the red and black lines, respectively. The error bars span the 5th to 95th percentiles.

(C) Mean sleep-onset latency (±1 SEM) in rocking and stationary conditions. For all panels, the red asterisks indicate significant differences (paired t test, $p < 0.05$, n = 9) between stationary (gray boxes and bar) and rocking (orange boxes and bar) conditions.

During rocking, the theta-dominated waking theta peak shifted toward lower frequencies in *Otop1*$^{+/+}$ and *Otop1*$^{+/tlt}$ mice, while the REM-sleep theta peak was reduced in *Otop1*$^{+/tlt}$ mice, but not in *Otop1*$^{+/+}$ mice (Figure 7B, right panel). The TPF of neither state was affected in *tilted* mice.

The findings in this second cohort of mice with functional otoliths confirm the results of the first experiments on B6 mice regarding the effect of 1.0-Hz rocking on wake-sleep distribution and EEG activity. The lack of rocking-induced changes in any of the variables measured in the *Otop1*$^{tlt/tlt}$ mice underscores the importance of the utricular and saccular input in the mediation of the effect.

DISCUSSION

The current study is the first to establish a rocking model in mice, demonstrating its effects on sleep distribution, architecture, and EEG activity in a species other than humans. We also experimentally validated the wide-held, but thus far unproven, notion that the rocking effects on sleep are mediated by the vestibular system. No measurable contribution from other modalities was observed, thereby underlining a functional connection between the otolithic organs and sleep circuitry. Our findings confirm that rocking decreases sleep-onset latency, increases NREM-sleep time, and reduces active wakefulness in mice, as in humans [3–5, 8]. Nevertheless, we did not find evidence of an enhanced NREM-sleep quality in mice, as has been reported in humans [22]. Lastly, although the evident similarities between *Otop1*$^{+/+}$ and *Otop1*$^{+/tlt}$ mice in all sleep variables measured here support previous observations that mice heterozygous for the *tlt* mutation form functional otoconial maculae, the notion of a gene-dosage effect reported for other behaviors such as performance on a balance task was not observed [23].

Rocking as Linear Acceleration in Mice and Humans

At least three previous studies in humans used rhythmic linear motion in the horizontal plane as their choice of rocking model [4, 5, 7]. However, their findings were not entirely consistent, most likely due to major methodological differences among the studies, such as the amplitude and frequency of the stimulations that were used. The firing rate of neurons encoding linear acceleration increases proportionally with the acceleration applied to the utricular hair bundles [24, 25], and, accordingly, rocking efficiency depends on the maximum linear acceleration applied [8]. The maximum linear acceleration (α_{max}) of a simple harmonic motion, such as rocking in the horizontal plane, depends on the frequency (or rate, *f*) of rocking and the maximum amplitude (or displacement, A_{max}) of motion, according to the function $\alpha_{max} = (2\pi f)^{2*}A_{max}$. Based on the frequencies and amplitudes reported in the human rocking studies, Woodward [4] applied a maximum linear acceleration of 22 cm/s^2 and Bayer [5] applied one of 26 cm/s^2, whereas the most recent study by Omlin [7] used accelerations of 15 cm/s^2 and lower. In the current study, rocking at 1.0 and 1.5 Hz resulted in accelerations of 79 and 178 cm/s^2, respectively. In support of the dependency of rocking efficacy on linear acceleration, the observed effects in the current study were consistently larger at 1.5 than at 1.0 Hz. More importantly, in a follow-up experiment, we demonstrated that the 1.0-Hz rate was optimal only at the 20-mm displacement, i.e., at an acceleration of 79 cm/s^2 (Figure S6). Rocking at 1.0 Hz with a smaller displacement (8 mm), and thus a lower acceleration (32 cm/s^2), did not affect sleep, while 1.0-Hz rocking with a 45-mm displacement recapitulated the effect on sleep of 1.5-Hz rocking with a 20-mm displacement, since both rocking conditions shared the same linear acceleration (178 cm/s^2; Figure S6).

Mouse vestibular afferents are 3–4 times less sensitive to stimuli than those in monkeys [26, 27] and in humans [28, 29]. Applying this conversion to our results yields as lowest maximum acceleration that affected sleep in mice (79 cm/s^2) values in the 20–26 cm/s^2 range, closely matching the accelerations that affected sleep in humans. Moreover, the maximum acceleration at which rocking failed to affect sleep in mice (32 cm/s^2) approximates (i.e., 8–11 cm/s^2) the accelerations used by Omlin and colleagues. The importance of linear acceleration in the vestibular encoding of rocking, underlined here, should be taken into

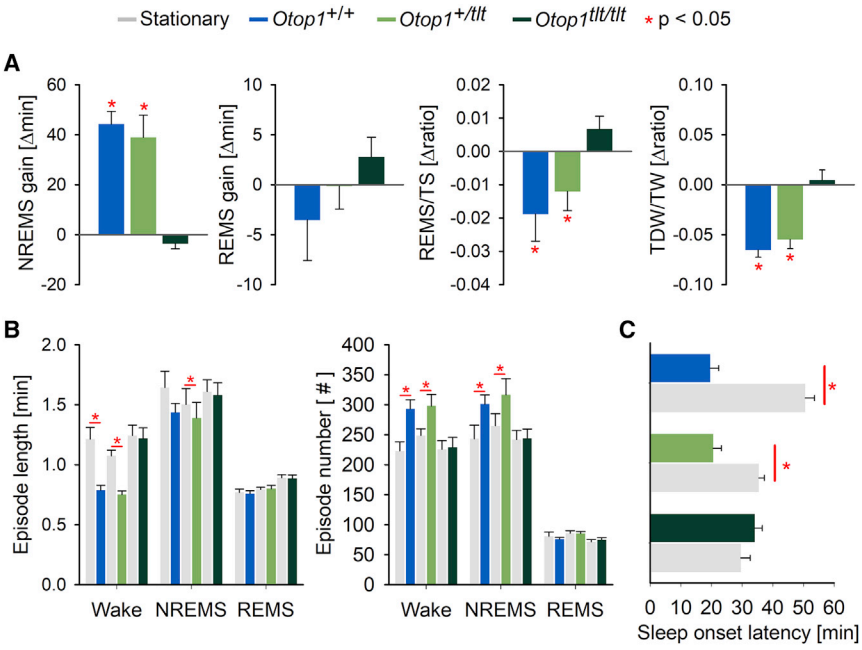

Figure 6. Rocking Does Not Affect Sleep in *Otop1*$^{tlt/tlt}$ Mice

(A) From left to right: mean (±1 SEM) rocking-stationary differences in time spent in NREM sleep (NREMS; for stationary 12-h amounts, see Figure S5A) and REM sleep (REMS; both in Δminutes), as well as REMS-to-total-sleep (REMS/TS) and theta-dominated-waking to-total-wakefulness (TDW/TW; both in Δratios), during the 12-h light period for *Otop1*$^{+/+}$ (n = 6), *Otop1*$^{+/tlt}$ (n = 8), and *Otop1*$^{tlt/tlt}$ (n = 9) mice. Also see Table S2 for absolute values in all states and genotypes.

(B) Average episode duration (in minutes, left) and number of uninterrupted episodes (right) in all 3 states during the 12-h light period for the 3 genotypes. Significant differences are marked by the red asterisks.

(C) Sleep-onset latency (in minutes) under rocking and stationary conditions for the 3 *Otop1* genotypes. In all panels, the gray bars represent the stationary condition and the colored bars represent the rocking condition; blue (*Otop1*$^{+/+}$), green (*Otop1*$^{+/tlt}$) and black (*Otop1*$^{tlt/tlt}$) error bars indicate 1 SEM, and red asterisks denote significant differences (1-way ANOVA, genotype, $p < 0.02$; post hoc paired t tests, $p < 0.05$).

consideration in future studies investigating the effects of rocking on sleep. Furthermore, it should be noted that the deeper brain structures receiving the encoded rocking signal may be stimulated twice within a rocking cycle, since the maximum acceleration is reached when displacement is also at its maximum.

The utilization of a linear rocking model, in conjunction with the *tilted* mice in our study, allowed for a precise evaluation of the otolithic contribution in the mediation of the rocking effect. While the participation of other modalities, such as other mechanosensory, proprioceptive, and visual systems, has been hypothesized in previous studies in humans [2, 30], no compensation was observed in *Otop1*$^{tlt/tlt}$ mice, leaving mainly the utricular afferents as the sole mediators of the effect. Given the results of our study, we believe that the contribution of the linear component plays a pivotal role in the mediation of the rocking effect on sleep, even in everyday life, where rocking is unlikely to be purely linear and is likely to engage the contribution of additional vestibular cues.

Vestibular Pathways to the Sleep Circuitry

In the current study, rocking promoted NREM sleep by facilitating wake-to-NREM sleep transitions, however without enhancing NREM-sleep consolidation. The contribution of REM sleep to total sleep was reduced by rocking, particularly at 1.5 Hz, due to a decrease in the initiation of REM-sleep episodes. Time spent in theta-dominated waking, a waking substate closely associated with motivated locomotor activity, was also reduced. Concomitantly, a rocking fingerprint—a persistent EEG-power shift toward lower theta frequencies—was present in mice with functional otoliths during total wakefulness, theta-dominated waking, and REM sleep at rocking rates promoting NREM sleep. Brainstem structures potentially mediating these effects will be discussed below.

The close interrelationship between the vestibular nuclei and sleep-inducing structures of the brain has been extensively studied [31, 32]. Direct vestibular influence to several brainstem structures linked to sleep regulation [33, 34], such as the pedunculopontine tegmentum nucleus (PPT), locus coeruleus, raphe nucleus, solitary tract nucleus, and, more recently, the orexigenic lateral hypothalamus, has been demonstrated [35–37]. Of those structures, the PPT is of particular interest, because it is an important component of the sleep circuitry [38] and because cholinergic projections from the PPT reach the septohippocampal theta generators [39, 40]. A substantial number of PPT cells have been reported to be vestibular only, responding exclusively to rotational and translational stimuli [41]. Input from the vestibular nuclei, through the PPT, has been shown to generate specifically type 2 (4–7 Hz), atropine-sensitive theta activity in awake rats [42, 43], which coincides with the theta frequencies with increased EEG power density in rocked mice ([44, 45], reviewed in [46]). Furthermore, chemogenetic manipulation of PPT neuronal subpopulations in the rat produced sleep and EEG phenotypes closely related to those observed in the current study [47]. More specifically, inhibition of glutamatergic neurons reduced wakefulness and increased NREM sleep, whereas activation of GABAergic neurons resulted in a mild suppression of REM sleep. Lastly, activation of cholinergic neurons suppressed NREM-sleep EEG in the 9–18-Hz range (as observed at 1.0- and 1.5-Hz rocking in B6 mice; also see Figure S2, middle panels) and increased transitions between wakefulness and sleep. We conclude that there are a considerable number of indications implicating the PPT in the mediation of the effects of rocking on sleep, although the exact nature of its contribution remains to be elucidated.

In conclusion, the results of the current study support previous observations on the effects of rocking on sleep and provide

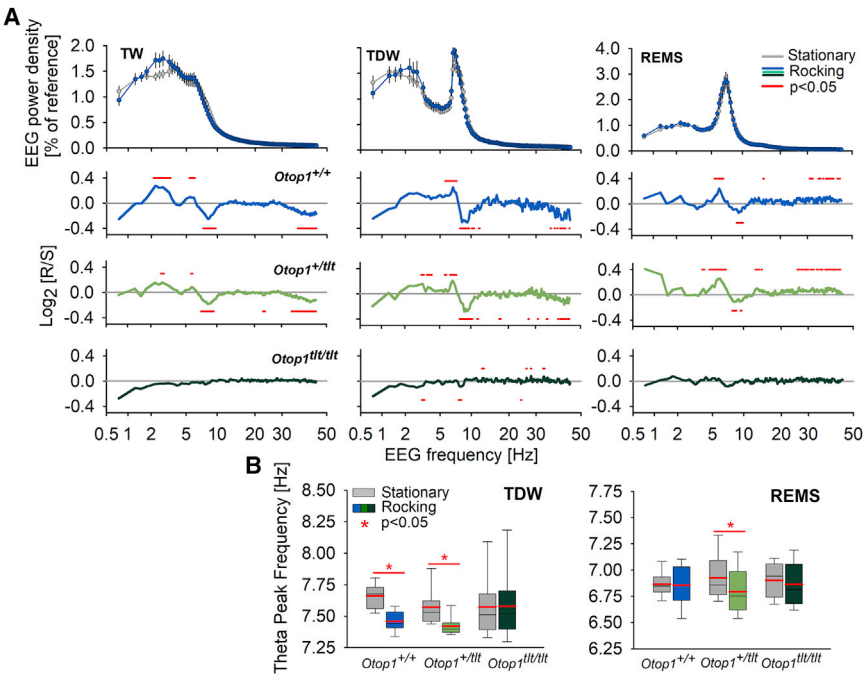

Figure 7. Rocking Affects Waking, Theta-Dominated Waking, and REM-Sleep EEG in Mice with Functional Otoliths

(A) From left to right: mean EEG spectral profiles (±1 SEM) of total wakefulness (TW), theta-dominated waking (TDW), and REM sleep (REMS) during the 12 h following light onset under stationary baseline (black line) and rocking (blue; 1.0 Hz) conditions for *Otop1*$^{+/+}$ mice. EEG power density is expressed as a percentage of baseline reference (S1 and S2; see STAR Methods). Relative changes are given in the 3 lower panels as the $\log_2$ of the rocking-to-stationary ratio (R/S; blue, *Otop1*$^{+/+}$; light green, *Otop1*$^{+/tlt}$; dark green, *Otop1*$^{tlt/tlt}$; gray, stationary). Values for the 1.0-, 2.0- and 3.0-Hz bins have been removed because of rocking artifacts in some mice (see STAR Methods). Statistical analyses were as follows: for TW (2-way rANOVA; *Otop1*$^{+/+}$, frequency × condition; *Otop1*$^{+/tlt}$, condition, frequency × condition; $p < 0.02$), for TDW (2-way rANOVA; *Otop1*$^{+/+}$, frequency × condition; *Otop1*$^{+/tlt}$, condition, frequency × condition; $p < 0.001$), and for REMS (2-way rANOVA; *Otop1*$^{+/+}$ and *Otop1*$^{+/tlt}$, condition, frequency × condition; $p < 0.05$). The red squares mark frequency bins in which rocking affected EEG power density (post hoc paired t tests, $p < 0.05$). For baseline NREM-sleep EEG spectral profiles, see Figure S5B.

(B) From left to right: theta peak frequency during TDW and REMS under rocking and stationary conditions for the 3 *Otop1* genotypes (see STAR Methods). The gray bars represent the stationary condition, while blue (*Otop1*$^{+/+}$, n = 6), light-green (*Otop1*$^{+/tlt}$, n = 8), and dark-green (*Otop1*$^{tlt/tlt}$, n = 9) bars represent the rocking condition. The mean and median of each group are indicated by the red and black lines within the boxplot, respectively. The red asterisks represent paired t tests (stationary versus rocking, $p < 0.05$). The error bars span the 5th to 95th percentiles.

insight to the mechanistic aspects of the phenomenon. Overall, our findings strengthen the view that the vestibular system can be utilized to promote NREM sleep, supporting efforts toward a non-pharmacological, non-invasive approach to aid patients suffering from sleep disorders.

STAR★METHODS

Detailed methods are provided in the online version of this paper and include the following:

- KEY RESOURCES TABLE
- CONTACT FOR REAGENT AND RESOURCE SHARING
- EXPERIMENTAL MODEL AND SUBJECT DETAILS
  - Animals and Housing Conditions
  - Experiment 1
  - Experiment 2
  - Experiment 3
- METHOD DETAILS
  - EEG/EMG Implantation
- QUANTIFICATION AND STATISTICAL ANALYSIS
- DATA AND SOFTWARE AVAILABILITY
  - Data Acquisition and Analysis

SUPPLEMENTAL INFORMATION

Supplemental Information includes six figures and two tables and can be found with this article online at https://doi.org/10.1016/j.cub.2018.12.007.

ACKNOWLEDGMENTS

This study was supported by the Swiss National Science Foundation (SNF CR31I3_149731 to S.S., M.M., and P.F., supporting K.K. and A.P.), the state of Vaud (supporting K.K., Y.E., J.H., and P.F.), and the state of Geneva (supporting S.S., M.M., and L.B.). We thank Marieke Hoekstra, Mathias Peuvrier, and Catherine Moret for their technical assistance.

AUTHOR CONTRIBUTIONS

The study was designed by P.F., L.B., S.S., and M.M.; K.K. was in charge of mouse breeding; K.K. and Y.E. performed the experiments; K.K., J.H., and P.F. analyzed data; and K.K., A.P., L.B., and P.F. wrote the manuscript.

DECLARATION OF INTERESTS

The authors declare no competing interests.

Received: June 6, 2018
Revised: October 29, 2018
Accepted: December 6, 2018
Published: January 24, 2019

REFERENCES

1. Korner, A.F., Guilleminault, C., Van den Hoed, J., and Baldwin, R.B. (1978). Reduction of sleep apnea and bradycardia in preterm infants on oscillating water beds: a controlled polygraphic study. Pediatrics *61*, 528–533.
2. Edelman, A.H., Kraemer, H.C., and Korner, A.F. (1982). Effects of compensatory movement stimulation on the sleep-wake behaviors of preterm infants. J. Am. Acad. Child Psychiatry *21*, 555–559.

3. Korner, A.F., Ruppel, E.M., and Rho, J.M. (1982). Effects of water beds on the sleep and motility of theophylline-treated preterm infants. Pediatrics *70*, 864–869.
4. Woodward, S., Tauber, E.S., Spielmann, A.J., and Thorpy, M.J. (1990). Effects of otolithic vestibular stimulation on sleep. Sleep *13*, 533–537.
5. Bayer, L., Constantinescu, I., Perrig, S., Vienne, J., Vidal, P.P., Mühlethaler, M., and Schwartz, S. (2011). Rocking synchronizes brain waves during a short nap. Curr. Biol. *21*, R461–R462.
6. Crivelli, F., Omlin, X., Rauter, G., von Zitzewitz, J., Achermann, P., and Riener, R. (2016). Somnomat: a novel actuated bed to investigate the effect of vestibular stimulation. Med. Biol. Eng. Comput. *54*, 877–889.
7. Omlin, X., Crivelli, F., Näf, M., Heinicke, L., Skorucak, J., Malafeev, A., Fernandez Guerrero, A., Riener, R., and Achermann, P. (2018). The effect of a slowly rocking bed on sleep. Sci. Rep. *8*, 2156.
8. Pederson, D.R., and Vrugt, D.T. (1973). The influence of amplitude and frequency of vestibular stimulation on the activity of two-month-old infants. Child Dev. *44*, 122–128.
9. Khan, S., and Chang, R. (2013). Anatomy of the vestibular system: a review. NeuroRehabilitation *32*, 437–443.
10. Berthoz, A., Pavard, B., and Young, L.R. (1975). Perception of linear horizontal self-motion induced by peripheral vision (linearvection) basic characteristics and visual-vestibular interactions. Exp. Brain Res. *23*, 471–489.
11. Niessen, M.H., Veeger, D.H., and Janssen, T.W. (2009). Effect of body orientation on proprioception during active and passive motions. Am. J. Phys. Med. Rehabil. *88*, 979–985.
12. Ornitz, D.M., Bohne, B.A., Thalmann, I., Harding, G.W., and Thalmann, R. (1998). Otoconial agenesis in tilted mutant mice. Hear. Res. *122*, 60–70.
13. Hurle, B., Ignatova, E., Massironi, S.M., Mashimo, T., Rios, X., Thalmann, I., Thalmann, R., and Ornitz, D.M. (2003). Non-syndromic vestibular disorder with otoconial agenesis in tilted/mergulhador mice caused by mutations in otopetrin 1. Hum. Mol. Genet. *12*, 777–789.
14. Vassalli, A., and Franken, P. (2017). Hypocretin (orexin) is critical in sustaining theta/gamma-rich waking behaviors that drive sleep need. Proc. Natl. Acad. Sci. USA *114*, E5464–E5473.
15. Welsh, D.K., Richardson, G.S., and Dement, W.C. (1985). A circadian rhythm of hippocampal theta activity in the mouse. Physiol. Behav. *35*, 533–538.
16. Franken, P., Dijk, D.J., Tobler, I., and Borbély, A.A. (1991). Sleep deprivation in rats: effects on EEG power spectra, vigilance states, and cortical temperature. Am. J. Physiol. *261*, R198–R208.
17. Borbély, A.A. (1982). A two process model of sleep regulation. Hum. Neurobiol. *1*, 195–204.
18. Dijk, D.J., Hayes, B., and Czeisler, C.A. (1993). Dynamics of electroencephalographic sleep spindles and slow wave activity in men: effect of sleep deprivation. Brain Res. *626*, 190–199.
19. Vyazovskiy, V.V., Achermann, P., Borbély, A.A., and Tobler, I. (2004). The dynamics of spindles and EEG slow-wave activity in NREM sleep in mice. Arch. Ital. Biol. *142*, 511–523.
20. Krystal, A.D., Zammit, G.K., Wyatt, J.K., Quan, S.F., Edinger, J.D., White, D.P., Chiacchierini, R.P., and Malhotra, A. (2010). The effect of vestibular stimulation in a four-hour sleep phase advance model of transient insomnia. J. Clin. Sleep Med. *6*, 315–321.
21. Jones, S.M., Erway, L.C., Johnson, K.R., Yu, H., and Jones, T.A. (2004). Gravity receptor function in mice with graded otoconial deficiencies. Hear. Res. *191*, 34–40.
22. Perrault, A.A., Khani, A., Quairiaux, C., Kompotis, K., Franken, P., Muhlethaler, M., Schwartz, S., and Bayer, L. (2019). Whole-Night Continuous Rocking Entrains Spontaneous Neural Oscillations with Benefits for Sleep and Memory. Curr. Biol. Published online January 24, 2019. https://doi.org/10.1016/j.cub.2018.12.028.
23. de Caprona, M.D., Beisel, K.W., Nichols, D.H., and Fritzsch, B. (2004). Partial behavioral compensation is revealed in balance tasked mutant mice lacking otoconia. Brain Res. Bull. *64*, 289–301.
24. Angelaki, D.E., Shaikh, A.G., Green, A.M., and Dickman, J.D. (2004). Neurons compute internal models of the physical laws of motion. Nature *430*, 560–564.
25. Jamali, M., Sadeghi, S.G., and Cullen, K.E. (2009). Response of vestibular nerve afferents innervating utricle and saccule during passive and active translations. J. Neurophysiol. *101*, 141–149.
26. Cullen, K.E. (2014). The neural encoding of self-generated and externally applied movement: implications for the perception of self-motion and spatial memory. Front. Integr. Nuerosci. *7*, 108.
27. Lasker, D.M., Han, G.C., Park, H.J., and Minor, L.B. (2008). Rotational responses of vestibular-nerve afferents innervating the semicircular canals in the C57BL/6 mouse. J. Assoc. Res. Otolaryngol. *9*, 334–348.
28. Carriot, J., Jamali, M., Chacron, M.J., and Cullen, K.E. (2017). The statistics of the vestibular input experienced during natural self-motion differ between rodents and primates. J. Physiol. *595*, 2751–2766.
29. Yu, X.J., Dickman, J.D., and Angelaki, D.E. (2012). Detection thresholds of macaque otolith afferents. J. Neurosci. *32*, 8306–8316.
30. Korner, A.F., Schneider, P., and Forrest, T. (1983). Effects of vestibular-proprioceptive stimulation on the neurobehavioral development of preterm infants: a pilot study. Neuropediatrics *14*, 170–175.
31. Bizzi, E., Pompeiano, O., and Somogyi, I. (1964). Vestibular nuclei: activity of single neurons during natural sleep and wakefulness. Science *145*, 414–415.
32. Morrison, A.R., and Pompeiano, O. (1970). Vestibular influences during sleep. VI. Vestibular control of autonomic functions during the rapid eye movements of desynchronized sleep. Arch. Ital. Biol. *108*, 154–180.
33. Yates, B.J., Grélot, L., Kerman, I.A., Balaban, C.D., Jakus, J., and Miller, A.D. (1994). Organization of vestibular inputs to nucleus tractus solitarius and adjacent structures in cat brain stem. Am. J. Physiol. *267*, R974–R983.
34. Murakami, D.M., Erkman, L., Hermanson, O., Rosenfeld, M.G., and Fuller, C.A. (2002). Evidence for vestibular regulation of autonomic functions in a mouse genetic model. Proc. Natl. Acad. Sci. USA *99*, 17078–17082.
35. Horowitz, S.S., Blanchard, J., and Morin, L.P. (2005). Medial vestibular connections with the hypocretin (orexin) system. J. Comp. Neurol. *487*, 127–146.
36. Semba, K., and Fibiger, H.C. (1992). Afferent connections of the laterodorsal and the pedunculopontine tegmental nuclei in the rat: a retro- and antero-grade transport and immunohistochemical study. J. Comp. Neurol. *323*, 387–410.
37. Besnard, S., Tighilet, B., Chabbert, C., Hitier, M., Toulouse, J., Le Gall, A., Machado, M.L., and Smith, P.F. (2018). The balance of sleep: role of the vestibular sensory system. Sleep Med. Rev. *42*, 220–228.
38. Datta, S., and Siwek, D.F. (1997). Excitation of the brain stem pedunculopontine tegmentum cholinergic cells induces wakefulness and REM sleep. J. Neurophysiol. *77*, 2975–2988.
39. Bland, B.H., and Oddie, S.D. (1998). Anatomical, electrophysiological and pharmacological studies of ascending brainstem hippocampal synchronizing pathways. Neurosci. Biobehav. Rev. *22*, 259–273.
40. Vertes, R.P., and Kocsis, B. (1997). Brainstem-diencephalo-septohippocampal systems controlling the theta rhythm of the hippocampus. Neuroscience *81*, 893–926.
41. Aravamuthan, B.R., and Angelaki, D.E. (2012). Vestibular responses in the macaque pedunculopontine nucleus and central mesencephalic reticular formation. Neuroscience *223*, 183–199.
42. Vanderwolf, C.H. (1975). Neocortical and hippocampal activation relation to behavior: effects of atropine, eserine, phenothiazines, and amphetamine. J. Comp. Physiol. Psychol. *88*, 300–323.
43. Aitken, P., Zheng, Y., and Smith, P.F. (2017). Effects of bilateral vestibular deafferentation in rat on hippocampal theta response to somatosensory stimulation, acetylcholine release, and cholinergic neurons in the pedunculopontine tegmental nucleus. Brain Struct. Funct. *222*, 3319–3332.
44. Tai, S.K., Ma, J., Ossenkopp, K.P., and Leung, L.S. (2012). Activation of immobility-related hippocampal theta by cholinergic septohippocampal neurons during vestibular stimulation. Hippocampus *22*, 914–925.

45. Shin, J. (2010). Passive rotation-induced theta rhythm and orientation homeostasis response. Synapse *64*, 409–415.

46. Aitken, P., Zheng, Y., and Smith, P.F. (2018). The modulation of hippocampal theta rhythm by the vestibular system. J. Neurophysiol. *119*, 548–562.

47. Kroeger, D., Ferrari, L.L., Petit, G., Mahoney, C.E., Fuller, P.M., Arrigoni, E., and Scammell, T.E. (2017). Cholinergic, glutamatergic, and GABAergic neurons of the pedunculopontine tegmental nucleus have distinct effects on sleep/wake behavior in mice. J. Neurosci. *37*, 1352–1366.

48. Mang, G.M., and Franken, P. (2012). Sleep and EEG phenotyping in mice. Curr. Protoc. Mouse Biol. *2*, 55–74.

49. Franken, P., Chollet, D., and Tafti, M. (2001). The homeostatic regulation of sleep need is under genetic control. J. Neurosci. *21*, 2610–2621.

50. Franken, P., Malafosse, A., and Tafti, M. (1998). Genetic variation in EEG activity during sleep in inbred mice. Am. J. Physiol. *275*, R1127–R1137.

51. Hughes, I., Blasiole, B., Huss, D., Warchol, M.E., Rath, N.P., Hurle, B., Ignatova, E., Dickman, J.D., Thalmann, R., Levenson, R., and Ornitz, D.M. (2004). Otopetrin 1 is required for otolith formation in the zebrafish Danio rerio. Dev. Biol. *276*, 391–402.

52. Kim, D., Hwang, E., Lee, M., Sung, H., and Choi, J.H. (2015). Characterization of topographically specific sleep spindles in mice. Sleep *38*, 85–96.

53. Ang, G., McKillop, L.E., Purple, R., Blanco-Duque, C., Peirson, S.N., Foster, R.G., Harrison, P.J., Sprengel, R., Davies, K.E., Oliver, P.L., et al. (2018). Absent sleep EEG spindle activity in GluA1 (Gria1) knockout mice: relevance to neuropsychiatric disorders. Transl. Psychiatry *8*, 154.

54. Niethard, N., Ngo, H.V., Ehrlich, I., and Born, J. (2018). Cortical circuit activity underlying sleep slow oscillations and spindles. Proc. Natl. Acad. Sci. USA *115*, E9220–E9229.

STAR★METHODS

KEY RESOURCES TABLE

REAGENT or RESOURCE	SOURCE	IDENTIFIER
Experimental Models: Organisms/Strains		
Mouse: C57BL6/J	In-house (Centre for Integrative Genomics)	n/a
Mouse: *Otop1*$^{tlt/tlt}$: B6.Cg-*Otop1*tlt/J	The Jackson Laboratory	JAX: 001104, RRID:MGI:3700197
Software and Algorithms		
Somnologica-3™	Medcare Flaga	N/A
TMT Pascal Multi-Target5	Framework Computers Inc.	https://www.frameworkpascal.com/download.htm
STATISTICA 8.0	StatSoft Inc.	http://www.statsoft.com/Products/STATISTICA-Features
SIGMASTAT 3.5	Systat Software Inc.	https://systatsoftware.com/products/sigmastat/
SIGMAPLOT 12.5	Systat Software Inc.	http://www.sigmaplot.co.uk/products/sigmaplot/sigmaplot-details.php
Sleep-state-amount algorithm	[48]	paul.franken@unil.ch
Theta-dominated-waking algorithm	[14]	paul.franken@unil.ch
Delta-power algorithm	[49]	paul.franken@unil.ch
Spectral-analysis algorithm	[49]	paul.franken@unil.ch
Theta-eak-frequency algorithm	[14, 50]	paul.franken@unil.ch
Sigma-surge-detection algorithm	This paper	jeffrey.hubbard@unil.ch
Other		
Reciprocating linear-motion platform HS 260 Control	IKA	Ident. No.: 0003066700
Motor for custom-made platform	Orientalmotor	Item # BLM5120P-GFV2
Digital driver for custom-made platform	Orientalmotor	Item # BMUD120-C2

CONTACT FOR REAGENT AND RESOURCE SHARING

Further information and requests for resources and reagents should be directed to the Lead Contact, Paul Franken (paul.franken@unil.ch).

EXPERIMENTAL MODEL AND SUBJECT DETAILS

Animals and Housing Conditions

C57BL6/J (B6) mice bred locally (Centre for Integrative Genomics, University of Lausanne) and C57BL/6J mice with a congenital mutation in the *Otop1* gene (B6.Cg-*Otop1*tlt/J), originally purchased from The Jackson Laboratory (Bar Harbor, USA) and then also bred locally, were used. B6.Cg-*Otop1*tlt/J homozygous (*Otop1*$^{tlt/tlt}$), heterozygous (*Otop1*$^{+/tlt}$), and wild-type (*Otop1*$^{+/+}$) mice were obtained by crossings of heterozygous mice. B6.Cg-*Otop1*tlt/J *tilted* (*Otop1*$^{tlt/tlt}$) mice are homozygous for a spontaneous recessive mutation (C476A in exon 3 resulting in Ala151Glu) in the *Otop1* gene [12, 13]. The encoded protein, Otopetrin 1, regulates the formation of calcium carbonate crystals, otoconia, in the inner ear, which are essential for the physiological function of the otolithic organs of the vestibular system [13, 51]. Wild-type (*Otop1*$^{+/+}$) or heterozygous (*Otop1*$^{+/tlt}$) mice both form a histologically healthy utricular and saccular epithelia, containing a full complement of otoconia, while *tilted* mice completely lack otoconia [12]. Genotyping of the B6.Cg-*Otop1*tlt/J mice was performed by Sanger sequencing (GATC Biotech AG, Switzerland) according to the protocol provided by The Jackson Laboratory.

During the experiments all mice were individually housed in cages (31 × 18 × 18 cm) in a sound attenuated and temperature/humidity controlled room (25°C and 50%–60%, respectively). Mice were kept under a 12h light/ 12h dark cycle (lights on at ZT0 = 8 AM, 70-90 lux) and had access to food and water *ad libitum*. All animal procedures followed Swiss federal law and were preapproved by the Ethical Committee of the State of Vaud Veterinary Office, Switzerland (license number VD2803).

Experiment 1

Animals, in their home cage, were placed on a reciprocating linear-motion platform (HS 260 Control, IKA, Switzerland), which provided motion along one axis in the horizontal plane, with a non-adjustable maximum displacement of ± 20mm at variable periodicity

(Figure 1A). The rocking rates tested were 0.25, 0.5, 1.0, and 1.5 Hz. Note that the rocking rates refer to the harmonic motion of the platform and not the stimulus encoded to the vestibular nuclei, which may be twice as frequent. EEG and EMG signals were recorded continuously for 96 hours for each rate experiment. During the first 48 of these 96 hours, which were considered as baseline, mice were left undisturbed with the platforms in stationary condition. Starting at light onset of the third day, animals were rocked at a constant rate for 12 hours (ZT0–ZT12). The remaining 36 hours starting at dark onset (ZT12) were again spent undisturbed (Figure 1B, Experiment 1). In a first experiment, all mice (n = 6) were rocked at 0.25 Hz; i.e., the rocking rate used in the human experiment by Bayer and colleagues [5]. Next, two new cohorts of mice (n = 4 and 6) were rocked independently at 0.5, 1.0, and 1.5 Hz. To control for potential order effects, we divided each cohort into two groups, each with a different sequence of rocking rates: 1.0, 0.5, and 1.5 Hz or 1.5 Hz, 0.5, and 1.0 Hz (n = 2 per group for the first cohort, and n = 3 per group for the second cohort), respectively. Each mouse was subjected to all three rocking rates. For each rate tested, the aforementioned four-day protocol was applied, with a period of three days between the end of the previous and the beginning of the next recording, i.e., 7 days between each rocking experiment.

Experiment 2

Effects of 1.0-Hz rocking on sleep onset latency were assessed using the same two cohorts of mice described above (n = 4 and 6) in a crossover design (see Figure 1B, Experiment 2). Sleep onset latency is difficult to ascertain in spontaneously sleeping mice, as many sleep bouts occur without a time reference to express sleep onset relative to. After the end of Experiment 1, mice were left undisturbed for two days. Subsequently, mice were divided into two groups, and four hours after light onset (ZT0–ZT4), they were sleep-deprived for one hour (ZT4–ZT5). Next, one group was rocked for the remaining 7 hours of the light period (ZT5–ZT12), while the other group remained stationary. The protocol was then repeated 36 hours later with the second group being rocked and the first kept stationary. Sleep onset latency was defined as the time elapsed between the end of the 1-hour sleep deprivation (ZT5) and the first appearance of consolidated NREM sleep, i.e., $\geq$ 1 min of NREM sleep not interrupted by more than two consecutive 4-s epochs of wakefulness.

The two experiments (Figure 1B, Experiments 1&2) were repeated at 1.0 Hz in B6.Cg-*Otop1*tlt/J mice homozygous, heterozygous, and wild-type for the mutation [i.e., $Otop1^{tlt/tlt}$ (n = 9), $Otop1^{+/tlt}$ (n = 8), and $Otop1^{+/+}$ (n = 6), respectively]. A total of 4 cohorts were recorded from 4 litters, containing all 3 genotypes in different ratios, in 4 separate sets of experiments (1&2). Each mouse participated in both experiments.

Experiment 3

To determine whether linear acceleration or rocking rate was responsible for the rocking effects on sleep, a third, follow-up experiment inspired by one of the reviewers of the manuscript (Experiment 3; Figure S6, black bars) was performed using C57BL6/J mice (n = 6) and a custom-made platform with variable displacement (ranging between 8, 20, and 45mm). The harmonic motion of the platform was achieved using a motor (BLM5120P-GFV2; Orientalmotor) controlled by a programmable digital driver (BMUD120-C2; Orientalmotor). The different displacements were achieved by changing the radius of rotation on an additional intermediate arm, attached to the platform's arm. The rocking rate was kept constant at 1.0 Hz, and mice were rocked at different displacements during the 12-hour light period. Each mouse was subjected once to all three displacements over the course of 3 weeks, first at 20mm, followed by 45mm and 8mm. Two stationary baseline days were recorded prior to each rocking day, and each rocking experiment was separated by 7 days.

METHOD DETAILS

EEG/EMG Implantation

Male mice, 10-12 weeks old, were implanted with electroencephalographic (EEG) and electromyographic (EMG) electrodes under deep anesthesia (Xylazine 10 mg/kg, Ketamine 100 mg/kg, intraperitoneally), as described previously [50]. A fronto-parietal bipolar derivation was used to record EEG activity from the mouse cortex. Briefly, two gold-plated miniature screws serving as EEG electrodes were positioned over the right cerebral hemisphere (fronto-parietal positions) while two gold wires serving as EMG electrodes were inserted into the trapezius (neck) muscles. The EEG and EMG electrodes were soldered to a connector and together with four anchor screws (over the right and left hemispheres) were cemented to the skull. Animals were allowed to recover from surgery for four to six days before they were connected to the recording leads. A minimum of six days of habituation to the cables and the experimental room was scheduled before data collection. In total, there was a minimum of 10 days between surgery and the start of recordings.

QUANTIFICATION AND STATISTICAL ANALYSIS

TMT Pascal Multi-Target5 software (Framework Computers Inc., Brighton, MA, USA) was used to manage the data, Sigmastat 3.5 (Systat Software Inc., Chicago, IL, USA) and STATISTICA 8.0 (StatSoft Inc., Tulsa, OK, USA) for statistical analyses, and SigmaPlot 12.5 (Systat Software Inc., Chicago, IL, USA) for graph generation. For all measured variables, values during rocking were contrasted to the averaged values of the two preceding stationary baselines, during the same time of day. To assess the effects of rocking rate

(for B6 mice) or genotype (for *Otop1* mice), and condition (rocking versus stationary) on the various sleep-wake variables (i.e., time spent in state, state transitions, EEG delta power, EEG spectra), 2-way repeated-measures analyses of variance (rANOVAs) were performed first. Significant effects were decomposed using post hoc paired t tests. Significance threshold was set to $p = 0.05$. Results are reported as mean ± SEM. All information regarding the statistical tests and number of animals used can be found in the respective Figure legends.

DATA AND SOFTWARE AVAILABILITY

Data Acquisition and Analysis

EEG and EMG signals were recorded using EMBLA hardware and Somnologica-3 software (Medcare Flaga, Iceland). The analog signals were digitized at 2 kHz and subsequently downsampled to 200 Hz. The EEG was subjected to a discrete Fourier transformation yielding power spectra (range analyzed: 0.75–90 Hz; frequency resolution: 0.25 Hz; window-size: 4 s; window function: Hamming). EEG power density in the 47.5-52.5 Hz band was discarded from further analysis because of power line artifacts in the EEG of some of the animals.

After data acquisition, sleep-wake states were visually determined for each 4-s epoch as REM sleep ("R"), NREM sleep ("N"), or wakefulness ("W") according to standard criteria [48]. Recordings containing non-rocking-related EEG/EMG artifacts were excluded from further analysis (*for state amounts*: $n_{0.5Hz} = 3$, $n_{1.0Hz} = 1$, $n_{1.5Hz} = 1$; *for EEG spectral analysis*: $n_{0.25Hz} = 3$, $n_{0.5Hz} = 3$, $n_{1.0Hz} = 2$, $n_{1.5Hz} = 1$). Epochs scored as W were algorithmically subdivided into waking epochs in which the EEG was dominated by clear theta (θ, 5.0-9.5 Hz) activity; i.e., theta-dominated waking (TDW; see [14] for details). Because only artifact-free W epochs could be taken into consideration for the TDW classification, time spent in TDW was adjusted for the relative presence of artifact-containing W epochs during a given recording period.

Time spent in each state was calculated for 1- and 12-hour intervals. NREM and REM sleep gains were calculated as the time-matched difference between time spent in the respective state during the rocking condition and the two stationary days. The difference between the rocking and stationary condition was calculated also for REM sleep, expressed as a fraction of total sleep (TS, i.e., NREM + REM sleep), and theta-dominated waking (TDW), as a fraction of total wakefulness (TW, i.e., TDW + non-TDW).

Mean EEG spectra was obtained for consecutive 0.25 Hz bins for each behavioral state (0.75-90 Hz). Interindividual differences in overall EEG signal power were normalized by expressing EEG spectral density in each frequency bin as a percentage of a baseline reference calculated as the mean total EEG power over all frequencies and behavioral states over the 48h of baseline. The relative contribution of the behavioral states to this individual reference value was weighted so as to avoid that, e.g., individuals that spent more time in NREM sleep (during which overall EEG power is higher compared to wake and REM sleep) obtain a higher reference power as a result. During rocking, some animals ($n_{0.25Hz} = 3$, $n_{0.5Hz} = 0$, $n_{1.0Hz} = 4$, $n_{1.5Hz} = 7$, $n_{Otop1}^{+/+} = 1$, $n_{Otop1}^{+/tlt} = 3$, $n_{Otop1}^{tlt/tlt} = 1$) displayed EEG artifacts in the frequency bin corresponding to the rocking rate, as well as in up to two harmonic frequency bins. The frequency bins concerned were omitted from spectral analyses for all animals, even those without rocking artifacts. The neighboring frequency bins were not affected by the rocking rate, as assessed by within subject comparisons to the stationary baseline EEG spectra.

The central or peak frequency of the theta oscillation characteristic of the EEG signal of TDW and REM sleep was determined as the frequency bin with maximum power density in the θ range for each 4-s epoch. Theta peak frequency (TPF) was then calculated as the average of all peak frequencies obtained for all 4-s epochs within individuals.

EEG delta power dynamics during the two conditions were analyzed as described previously [49]. In short, EEG delta power was calculated as the average power density in the 1.0–4.0 Hz range in 4-s epochs scored as NREM sleep. Each 12-hour period of the four day recording was divided into segments (12 for light and 6 for dark period) to which an equal number of NREM sleep epochs contributed (i.e., percentiles). Since we were strictly interested in the sleep-wake dependent changes in EEG delta power, values were expressing as percentage of the mean EEG delta power over the last 4 hours of the two baseline light periods when lowest and stable levels are reached.

Sleep onset latency was calculated as the difference between the end of the 1-hour sleep deprivation and the first uninterrupted NREM sleep episode with a duration over 15 4-s epochs. Episode duration was calculated as the average length of uninterrupted episodes of wakefulness, NREM, or REM sleep during ZT0–ZT12. Episode number was calculated as the average count of uninterrupted episodes of a minimum of two 4-s epochs (> 8 s) of each one of the three sleep-wake states during ZT0–ZT12.

The sigma-surge detection algorithm was based on a combination of previously published methods for spindle-like-event detection [19, 52–54]. Briefly, fronto-parietal EEG signals, sampled at 200Hz, were filtered to the sigma band (10-16Hz), using a Chebyshev Type II filter (MATLAB function: Chebyshev), with cutoff frequencies of 8- and 18Hz. Only NREM sleep episodes of at least 12 s were included in the analysis. Next, to calculate instantaneous amplitude, a Hilbert transformation was applied to the filtered signal (MATLAB function: Hilbert), which was further smoothed to determine the signal envelope using a Gaussian filter with a 1-s window (MATLAB function: smoothdata with Gaussian modifier). As absolute EEG amplitude during NREM sleep varied across time and among individuals, a lower threshold was calculated as the mean amplitude of the envelope across each NREM-sleep episode (background noise) and subtracted from the rectified signal. A sigma surge started when signal envelope positively crossed this threshold and ended when a negative crossing was identified. A second threshold was set at 2.5x the standard deviation of the

background noise envelope based on visual observations of NREM-REM sleep transitions during baseline, in line with other detection algorithms [18]. Among crossings of this second threshold during a sigma surge a local maximum was determined (Figure S3A). Sigma-surge duration was constrained to successive positive and negative crossings of the lower threshold that lasted greater than 0.4 and less than 2.0 s. Total number of detected events, density, and average duration were consistent with previous studies [19, 53, 54]. To determine the timing of inter-surge intervals (Figure S3D), the distance between sigma surges was calculated for each NREM-sleep episode, which was then averaged across the entire period (either baseline or rocking) for each animal.